Earth Planets Space, **53**, 619–625, 2001

Evidence for an extended reconnection line at the dayside magnetopause

T. D. Phan[1], M. P. Freeman[2], L. M. Kistler[3], B. Klecker[4], G. Haerendel[4], G. Paschmann[4], B. U. Ö. Sonnerup[5], W. Baumjohann[4], M. B. Bavassano-Cattaneo[6], C. W. Carlson[1], A. M. DiLellis[6], K.-H. Fornacon[7], L. A. Frank[8], M. Fujimoto[9], E. Georgescu[4,10], S. Kokubun[11], E. Moebius[3], T. Mukai[12], W. R. Paterson[8], and H. Reme[13]

[1]*Space Sciences Laboratory, University of California, Berkeley, CA 94720, U.S.A.*
[2]*British Antarctic Survey, Cambridge, CB3 OET, United Kingdom*
[3]*Space Science Center, University of New Hampshire, NH 03824, U.S.A.*
[4]*Max-Planck-Institut für extraterrestrische Physik, 85740 Garching, Germany*
[5]*Thayer School of Engineering, Dartmouth College, Hanover, NH 03755, U.S.A.*
[6]*IFSI-CNR, 00133 Roma, Italy*
[7]*Technische Universität Braunschweig, 38106 Braunschweig, Germany*
[8]*Department of Physics and Astronomy, University of Iowa, Iowa City, IA 52242, U.S.A.*
[9]*Department of Earth and Planetary Sciences, Tokyo Institute of Technology, Meguro 152-8551, Japan*
[10]*Institute of Space Sciences, Bucharest, Romania*
[11]*Solar-Terrestrial Environment Laboratory, Nagoya University, Aichi 442-8507, Japan*
[12]*The Institute of Space and Astronautical Science, Sagamihara, Kanagawa 229-8510, Japan*
[13]*Centre d'Etude Spatiale des Rayonnements, Université Paul Sabatier, Toulouse, France*

(Received May 25, 2000; Revised November 7, 2000; Accepted November 27, 2000)

We report in-situ detection by two spacecraft of oppositely directed jets of plasma emanating from a magnetic reconnection site at the Earth's dayside magnetopause, confirming a key element inherent in all reconnection scenarios. The dual-spacecraft (Equator-S and Geotail) observations at the flank magnetopause, together with SuperDARN Halley radar observations of the subsolar cusp region, reveal the presence of a rather stable and extended reconnection line which lies along the equatorial magnetopause. These observations were made under persistent southward interplanetary magnetic field (IMF) conditions, implying that under these conditions the reconnection sites are determined by the large-scale interactions between the solar wind magnetic field and the dayside magnetosphere, rather than by local conditions at the magnetopause. Control by local conditions would result in patchy reconnection, distributed in a less well-organized fashion over the magnetopause surface.

1. Introduction

Magnetic reconnection is a universal plasma process which converts stored magnetic energy into kinetic and thermal energies. The process is thought to be important in many astrophysical contexts such as solar flares (Giovanelli, 1946; Masuda *et al.*, 1994; Yokoyama and Shibata, 1995) and solar coronal heating (Innes *et al.*, 1997); planetary magnetopauses and tails; cometary tails (Niedner *et al.*, 1981); and accretion disks.

The Earth's magnetosphere provides a unique opportunity to study the reconnection process from in-situ measurements. At the Earth's dayside magnetopause, high speed plasma jets of up to 1000 km/s—faster than the upstream solar wind flow speed—have been detected by single spacecraft traversing the magnetopause. For a number of events, the observed flow accelerations have been found to be in good agreement with reconnection theory (Paschmann *et al.*, 1979; Sonnerup *et al.*, 1981; Gosling *et al.*, 1986). These observations provided evidence that the plasma inside the magnetopause receives its high velocity from the magnetic kink resulting from the linkage between magnetosheath and magnetospheric fields. However, bi-directional jets—a key prediction of reconnection theory—have never been unambiguously observed and can in fact be seen from a single spacecraft only if the reconnection site happens to move past it. Without observational confirmation of the occurrence of bi-directional jets, the verification of the reconnection model, as it applies to the magnetosphere, remains incomplete.

Furthermore, with single-point measurements, the in-situ view of reconnection remains myopic: its location and scale size cannot be inferred. Without this knowledge, it has not been possible to deduce the large-scale properties and consequences of reconnection from observations at the magnetopause. Are the reconnection sites, their extent and the amount of energy transfer controlled by global boundary conditions or by local plasma conditions? If reconnection is initiated and maintained by large-scale interactions between the solar wind and the magnetosphere, the location, orientation, and extent of the X-line should be determined by the orientation of the interplanetary magnetic field (IMF). For example, for purely southward IMF, models of large-scale reconnection assume a reconnection line situated along

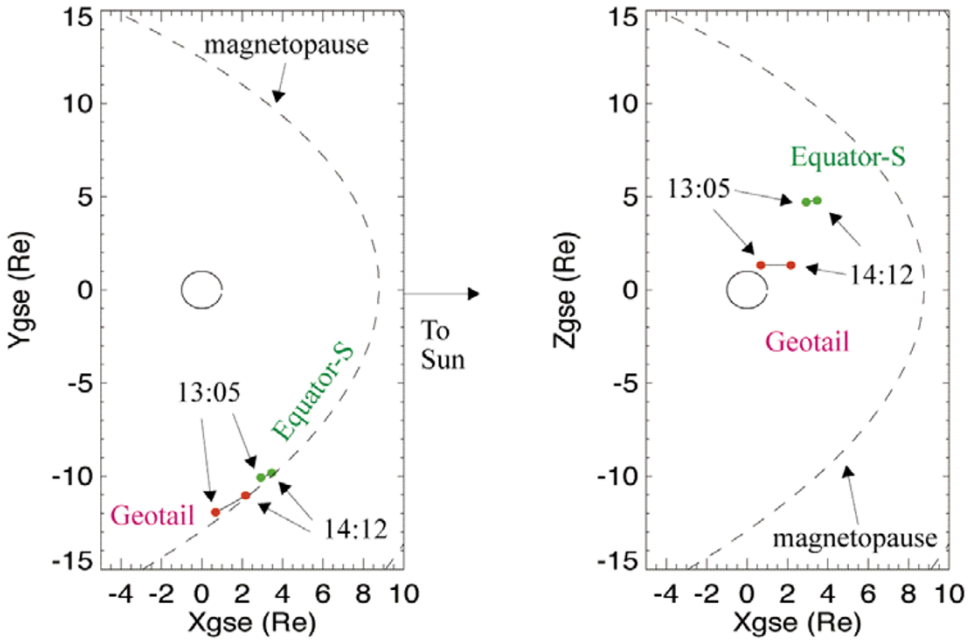

Fig. 1. Trajectories of Equator-S and Geotail on February 11, 1998 at 13:05 UT–14:12 UT. Left panel shows the orbits in the Ecliptic plane. Right panel displays the noon-midnight plane. The spacecraft separation was ~4 R_E in the north-south and ~3 R_E in the east-west direction.

the dayside equatorial magnetopause (Gonzales and Mozer, 1974; Sonnerup, 1974; Crooker, 1979), an assumption that has never been verified from in-situ observations. Reconnection controlled by local plasma conditions, on the other hand, would result in reconnection patches that are more randomly distributed over the magnetopause surface.

In this paper we report in-situ dual-spacecraft observations of bi-directional plasma jets at the magnetopause. These observations, together with SuperDARN radar observations, also provide evidence for a stable reconnection line extended along the dawn flank magnetopause. The bulk of the spacecraft observations presented here have been reported in *Nature* by Phan *et al.* (2000).

2. Spacecraft Orbits and Instrumentations

The Equator-S, Geotail, and Wind satellites are members of a fleet of spacecraft in the Inter-Agency Solar Terrestrial Physics Program (IASTP). The IASTP is designed to study solar-terrestrial interactions by providing simultaneous multi-point particle and field measurements of the Earth's magnetosphere and the surrounding interplanetary medium. For more than one hour on February 11, 1998, the trajectories of both the Equator-S and the Geotail spacecraft skimmed the dawn flank magnetopause (see Fig. 1). The spacecraft separation was ~4 Earth radii (R_E) in the north-south and ~3 R_E in the east-west direction. Continuous solar wind measurements were made by the Wind spacecraft at ~230 R_E upstream of the magnetopause.

The present study uses Equator-S plasma data obtained by the Ion Composition Instrument (Kistler *et al.*, 1999) with a temporal resolution of 3 seconds. Geotail plasma data are taken from the Low Energy Particle instrument (Mukai *et al.*, 1994) (at 3 s resolution) for the magnetosphere and magnetopause intervals and from the Comprehensive Plasma Instrument (Frank *et al.*, 1994) (at 20 s resolution) for the magnetosheath intervals adjacent to the magnetopause. The magnetic field is measured at a rate of 128 samples/s for Equator-S (Fornacon *et al.*, 1999) and 16 samples/s for Geotail (Kokubun *et al.*, 1994), but for our analysis the magnetic field data from both spacecraft are averaged over 3 seconds.

The boundary normal (LMN) coordinate system is used in this paper. It is defined such that the N axis points outward along the magnetopause normal and the (L, M) plane is tangential to the magnetopause with L oriented approximately due north and M due west (see Fig. 4). The magnetopause normal is taken from the Fairfield (1971) magnetopause model.

3. Observations

Figures 2(a)–(f) shows Equator-S and Geotail plasma and magnetic field data for the 13:05 UT–14:12 UT interval which reveal the presence of bi-directional jets. During this entire interval, Wind measured persistent southward IMF (Fig. 2(g)).

Equator-S. Panels (a)–(c) show multiple crossings of the magnetopause as the Equator-S orbit skimmed the magnetopause. High speed northward directed plasma flows ($V_L > 0$) were observed at many of these crossings. The flows in the magnetopause were enhanced in the northward direction by 200–300 km/s, relative to the magnetosheath flows detected adjacent to the magnetopause where $V_L \sim 30$ km/s (Panel (c)).

Geotail. The Geotail spacecraft, located ~4 R_E southward and ~3 R_E tailward of Equator-S, also crossed the magnetopause multiple times (Panels (d)–(f)). But in contrast to the jets encountered by Equator-S, those detected by Geotail were mostly in the southward direction: V_L was negatively enhanced by 200–300 km/s (Panel (d)).

To highlight the contrast in the flow directions detected by the two spacecraft, northward (southward) flow speed en-

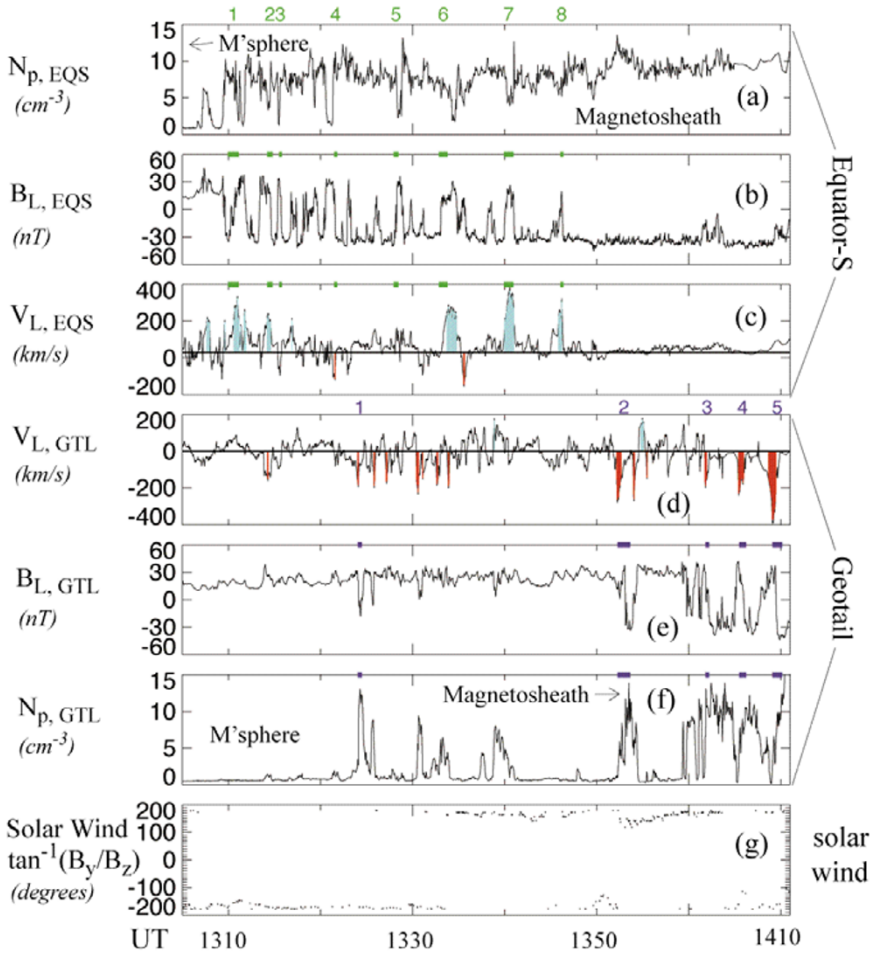

Fig. 2. Overview of multiple crossings of the magnetopause by Equator-S and Geotail. Panels (a)–(c) show the plasma density, L component of the magnetic field in the LMN boundary normal coordinate system, and the L component of the flow velocity, respectively, measured by Equator-S. Panels (d)–(f) display the L component of the flow velocity and the magnetic field, and the plasma density, respectively, measured by Geotail. The magnetopause encounters are identified by the transition between high density and southward magnetic field ($B_L < 0$) magnetosheath and low density and northward magnetic field magnetosphere. The green (purple) numbers at the top of panel (a) (panel (d)) denote the locations of complete magnetopause crossings. Northward (southward) flow enhancements larger than 150 km/s are shaded blue (red). Panel (g) shows the clock angle $\theta = \tan^{-1}(B_y/B_z)$ of the solar wind magnetic field measured by Wind. A forward time-shift of 45 minutes has been applied to the solar wind data to take into account the solar wind convection time from the Wind spacecraft position to the flank magnetopause. The field was strongly southward ($\theta \sim \pm 180^\circ$) during the entire interval.

hancements of greater than 150 km/s are shaded blue (red). Nine of the 11 Equator-S high-speed flow events are northward directed while 14 of 16 Geotail events are southward directed. Thus for the majority of cases, the reconnection site was located south of Equator-S and north of Geotail. The 4 exceptions (2 from each spacecraft) presumably correspond to instances when the reconnection site was either north or south of both spacecraft.

While Equator-S was mostly in the magnetosheath during this period and made only brief excursions into the magnetosphere, Geotail was in the reversed situation. This implies that, except for small short-term inward or outward motions, the magnetopause position was relatively stable. The observed brief encounters with plasma jets are the likely result of such motions causing the spacecraft to enter briefly into a region of longer duration jets. The fact that northward and southward jets do not appear simultaneously in Fig. 2 is also a direct consequence of the inward/outward magnetopause motion.

Solar Wind. Panel (g) displays the IMF clock angle in the plane perpendicular to the sun-Earth line, $\theta = \tan^{-1}(B_y/B_z)$, and in the geocentric solar magnetospheric coordinate system, measured by the Wind spacecraft at ~230 R_E upstream of the magnetopause. During the entire interval when the accelerated flows were observed, the IMF was almost purely southward: $\theta \sim \pm 180^\circ$.

4. Quantitative Comparisons with Theoretical Predictions of Reconnection

To establish that the jets are indeed the result of connection between magnetosheath and magnetospheric magnetic fields, we compare the plasma velocity enhancements observed in the magnetopause crossings with theoretical predictions.

Theory. According to magnetohydrodynamic models of reconnection at the dayside magnetopause involving weak magnetic field and high density plasma on the magnetosheath side and strong magnetic field and low density on the magnetospheric side, the reconnecting magnetopause can be described as a rotational discontinuity (Levy *et al.*, 1964). Across this discontinuity, the magnetosheath plasma is ac-

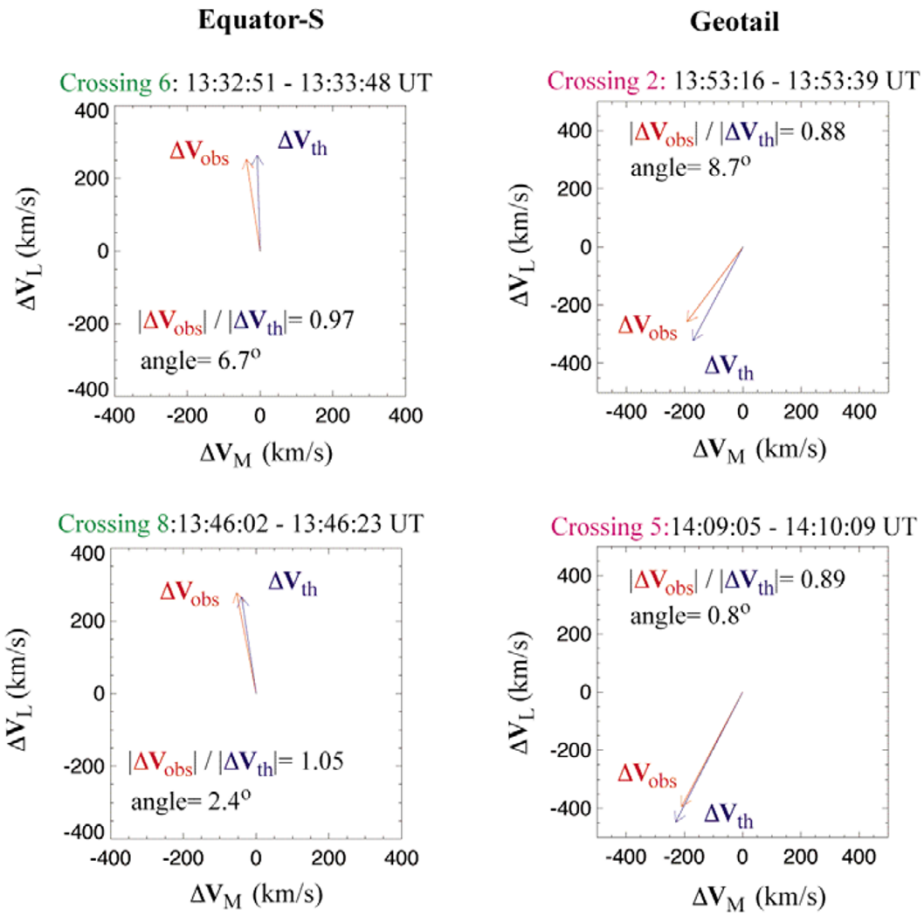

Fig. 3. Observed ($\Delta \mathbf{v}_{obs}$) and theoretical prediction ($\Delta \mathbf{v}_{th}$) of tangential (L, M) flow acceleration across the magnetopause for Equator-S crossings 6 and 8 (left panels) and Geotail crossings 2 and 5 (right panels). Note the remarkable agreements between predicted and observed flow accelerations.

celerated by the magnetic field tension force according to the following relation (Hudson, 1970):

$$\mathbf{v}_{t2} - \mathbf{v}_{t1} = \pm((1-\alpha_1)/\mu_0\rho_1)^{1/2}[(\rho_1/\rho_2)\mathbf{B}_{t2} - \mathbf{B}_{t1}]. \quad (1)$$

Here **B**, **v**, and ρ are the magnetic field vector, the plasma flow velocity, and the mass density, respectively. $\alpha \equiv (P_\parallel - P_\perp)/|\mathbf{B}|^2$ is the pressure anisotropy factor with $P_\parallel$ and $P_\perp$ being the plasma pressures parallel and perpendicular to the magnetic field, respectively. The subscript t denotes the component tangential to the magnetopause surface, while the subscript pair (1, 2) refers to the magnetosheath and the magnetospheric sides of the magnetopause. The choice of a positive or a negative sign on the right hand side of Eq. (1) depends on whether the observation point is north or south of the reconnection site. Equation (1) has been used in previous studies to deduce the presence of reconnection flows at the dayside magnetopause. However, it should be kept in mind that this relation is highly idealized since it is derived for a 1-D time stationary magnetopause, whereas the actual magnetopause exhibits 2-D and 3-D time-varying structures. Thus one should not expect perfect agreement between theory and observations.

Analysis. To simplify the analysis, we select only crossings in which the magnetic field exhibited a complete transition from its magnetosheath to its magnetospheric orientation. In total, there are 8 such crossings by Equator-S and 5 by Geotail. The times of these crossings are indicated in Fig. 2 along the top of the panels by green numbers and bars for the Equator-S events and by purple numbers and bars for the Geotail crossings.

The results of the analysis are illustrated in detail in Fig. 3 for four crossings—two from each spacecraft. Each panel of Fig. 3 shows the observed flow acceleration, $\Delta \mathbf{v}_{t,obs} = \mathbf{v}_{t2,obs} - \mathbf{v}_{t1,obs}$, together with the predicted tangential flow acceleration vector, $\Delta \mathbf{v}_{t,th}$, based on the densities and the components of the magnetic field tangential to the magnetopause (L, M) on the 2 sides the magnetopause. The predicted flows are computed from Eq. (1) using the positive sign for Equator-S and the negative sign for Geotail because of their observed northward and southward flow accelerations. For these events, the magnetosheath magnetic field and velocity samples (subscript 1 in Eq. (1)) are taken immediately adjacent to the magnetopause. The samples corresponding to subscript 2 in Eq. (1) are taken at the location of maximum observed flow acceleration, $|\Delta \mathbf{v}_{t,obs}|$. At this location the magnetic field has generally completed most (>80%) of its rotation to the magnetospheric value, thus it corresponds approximately to the magnetospheric edge of the magnetopause (Paschmann *et al.*, 1986).

The top-left panel of Fig. 3 shows the results for Equator-S crossing 6. The agreement between theory and observations is remarkable: The magnitude of the velocity increase is

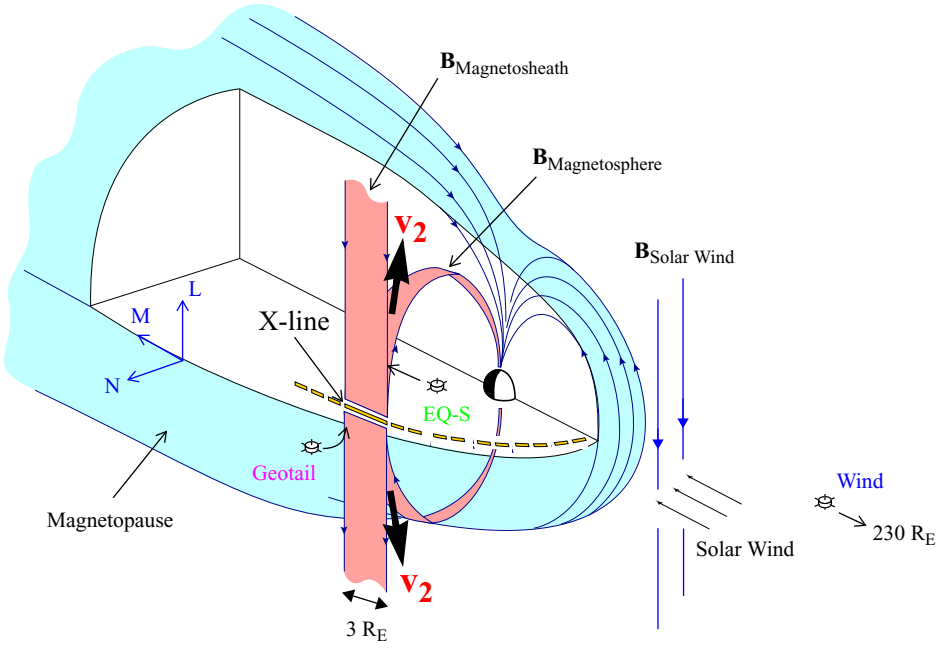

Fig. 4. 3-D cutaway view of the magnetosphere showing (1) the presence of bi-directional plasma jets ($\mathbf{v}_2$) as the result of reconnection between magnetosheath and dayside magnetospheric magnetic fields, and (2) the directly measured reconnection X-line (yellow solid line) along the dawn flank magnetopause and slightly north of the equatorial plane. The SuperDARN observations indicate that the complete X-line (yellow dashed line) extends to the subsolar point and over to the dusk flank. Also shown is the boundary normal (LMN) coordinate system.

97% of the predicted value, while the flow direction agrees to within 7°. For the Equator-S crossing 8 (bottom left panel), the agreement is equally remarkable. The flow speed increase agrees to within 5% and the direction to 2.4°.

For Geotail crossings 2 and 5 (right panels), the magnitude agreements of 88% and 89%, together with direction agreements of 8.7° and 0.8° for the two events also indicate excellent agreement with Eq. (1).

If one includes all crossings, the average magnitude agreement is 78% for the 8 Equator-S events and 74% for the 5 Geotail events. The corresponding average angle discrepancies are 3.8° and 6.1°. Among the events, there is one (Equator-S Crossing 5) where the observed flow acceleration $\Delta v_L < 100$ km/s was substantially below the prediction of $\Delta v_L \sim 380$ km/s. All other crossings displayed flow enhancements whose magnitudes were at least 50% of the prediction, and whose directions agreed to better than 10°. Taking this kind of agreement with theory as adequate evidence for reconnection (Sonnerup *et al.*, 1981), one concludes that all but one magnetopause crossing seen by both spacecraft had flow signatures consistent with reconnection.

5. The Big Picture

The combined Equator-S and Geotail observations of reconnection jets allow us to deduce the location, orientation, and minimum length of the reconnection line as illustrated in Fig. 4. With few exceptions, the two spacecraft detected oppositely directed jets which implies that the reconnection site (or X-line) must have been between the spacecraft, and therefore somewhat north of but not far from the equatorial plane. The X-line was oriented along the east-west direction because the jets were directed mainly in the north-south direction (Fig. 3). The repeated encounters of the jets over more than one hour imply that reconnection was active much of the time with its site remaining quasi-stationary.

The length of the X-line must have been at least 3 R_E along the flank magnetopause because of the spacecraft separation in the east-west direction. Although the full extent of the X-line is not directly measured, we infer from its persistent presence on the dawn flank, and from the frequent detection of quasi-steady reconnection jets in the subsolar region when the solar wind magnetic field is southward (e.g., Sonnerup *et al.*, 1981; Paschmann *et al.*, 1986), that the X-line must have extended to the subsolar region, and for symmetry reasons, all the way across to the dusk flank. Indeed, evidence that reconnection did occur in the subsolar region was obtained from SuperDARN radar (Greenwald *et al.*, 1995) observations, in the forms of equatorward motion of the cusp and poleward plasma flows across the polar cap boundary.

Figure 5 shows observations from the SuperDARN radar at Halley, Antarctica, during the 12:50 UT–14:10 UT interval. The radar field of view covers the 10 LT–11 LT range. Panel (a) shows the spectral width as a function of magnetic latitude and UT. High spectral width (>250 m/s) has been shown to be a proxy of the cusp (Baker *et al.*, 1995) resulting from enhanced wave activities in this region (André *et al.*, 1999). The present observations indicate that at 12:50 UT the cusp was located at magnetic latitude ~78°. During the next hour, the cusp moved steadily equatorward, reaching 72° by 14:00 UT. Since the equatorward boundary of the cusp corresponds to the separatrix between open and closed magnetic field lines, the steady equatorward motion of the cusp is evidence of a continuous increase in open magnetic flux due to quasi-steady reconnection at the dayside magnetopause at a greater

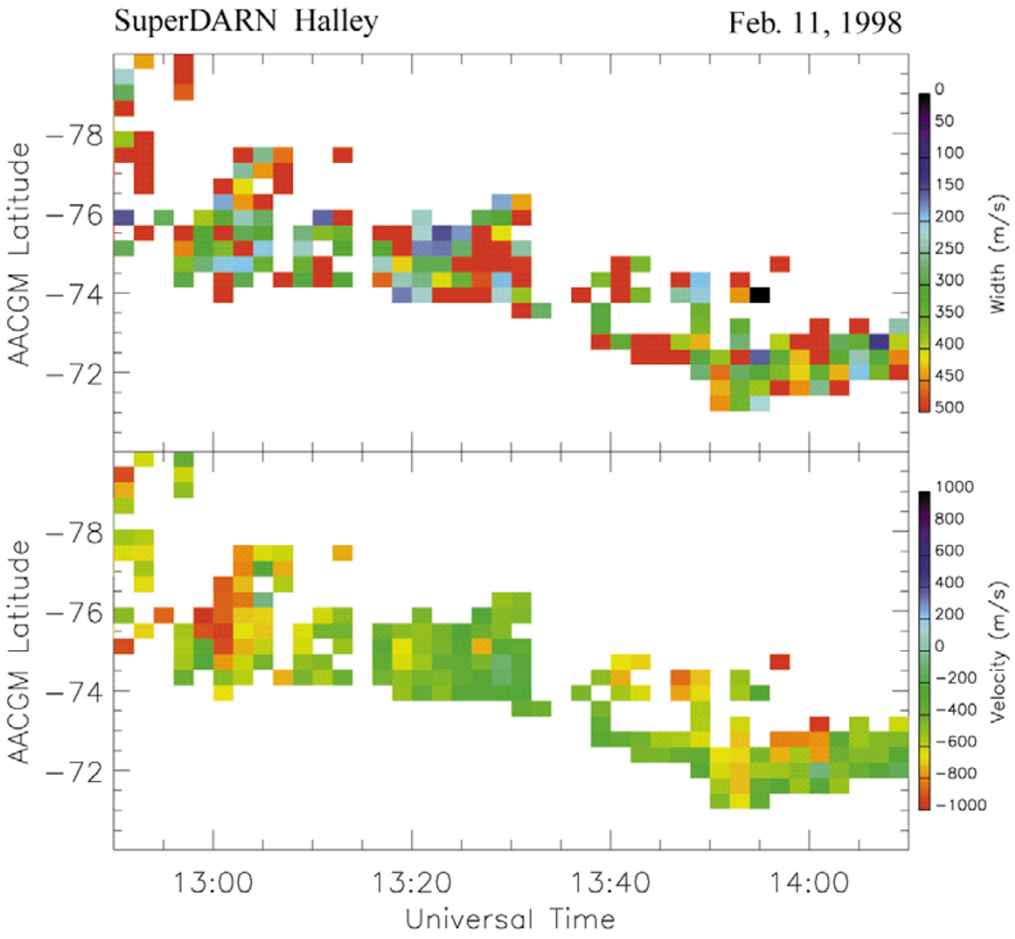

Fig. 5. Evidence for subsolar reconnection from observations of the cusp by the SuperDARN radar at Halley, Antarctica, covering the interval of Geotail and Equator-S magnetopause observations shown in Fig. 2. (a) Spectral width as a function of altitude-adjusted corrected geomagnetic latitude (AACGM) and universal time (UT). High spectral width (>250 m/s) is a proxy of cusp position. (b) line-of-sight plasma flow velocity as a function of AACGM and UT along a poleward-directed radar beam. Negative velocity corresponds to poleward flow.

rate than in the magnetotail (Siscoe and Huang, 1985). It is thus the ionospheric signature of dayside magnetopause erosion (Aubry *et al.*, 1970).

The reconnection rate at the radar local time can be estimated by measuring the convection electric field in the rest frame of the moving equatorward boundary of the cusp. Figure 5(b) shows the poleward component of $\mathbf{E}\times\mathbf{B}$ drift velocity measured by the Halley radar. The flows in the high spectral width cusp region are of ∼500 m/s or more, equivalent to an electric field of ∼25 mV/m in the rest frame of the Earth. Taking into account the equatorward motion of the cusp of ∼150 m/s, the reconnection electric field in the ionosphere is ∼33 mV/m or 15 kV per hour of MLT. Additional data from SuperDARN radars in the northern hemisphere (not shown) provide evidence that the projection of the magnetopause X-line extends from ∼9 MLT to at least 15 MLT, indicating a reconnection produced potential in excess of ∼90 kV. This value should be compared to the expected polar cap potential which represents the total magnetic flux transported from the dayside to the nightside magnetosphere by all processes, including viscous interaction (Axford and Hines, 1961) and reconnection. For the solar wind conditions at hand (from Wind spacecraft: V_{SW} = 550 km/s and B_{SW} = 7 nT, due south) the polar cap potential is predicted from an empirical relation based on a large assembly of low-altitude satellite data (Burke *et al.*, 1999), to be about 105 kV. Thus this crude analysis indicates that reconnection is indeed the dominant solar wind entry process when the IMF is persistently southward, with other processes playing at most a minor role.

6. Summary and Conclusion

In summary we have reported the first in-situ detections of bi-directional plasma jets which provide perhaps the most convincing evidence to-date of the occurrence of quasi-steady reconnection in space. We have also shown evidence for a stable equatorial reconnection line which implies that reconnection occurs in a large-scale rather than patchy and random manner under steady southward IMF conditions, and that its sites are determined by the large-scale interaction between the solar wind and the dayside magnetosphere rather than by local conditions at the magnetopause. Control by local conditions would result in patchy reconnection, distributed in a less well-organized fashion over the magnetopause surface.

The observations presented in this paper were made under the simple purely southward solar wind magnetic field geometry where most large-scale models of magnetopause reconnection predict an equatorial reconnection line (e.g.,

Dungey, 1961; Gonzales and Mozer, 1974; Sonnerup, 1974; Crooker, 1979), as observed. For other field orientations, the location and extent of the reconnection region are presently not known. Their predictions are model dependent. To evaluate which of the models (e.g., "component reconnection" (Gonzales and Mozer, 1974; Sonnerup, 1974) versus "antiparallel reconnection" (Crooker, 1979)) best represents the global reconnection configuration requires the identifications of the reconnection sites for a variety of field orientations, a task that could be performed by the four-spacecraft Cluster II mission.

Acknowledgments. We thank Ron Lepping, the principal investigator for the WIND MFI experiment, for making his magnetic field data and calibration available. We thank Arjun Raj, Harald Kucharek, Dimple Patel, and Peter Schroeder for their help in the processing of ESIC data. We also thank Marit Øieroset for her helpful comments on the manuscript. This research was funded by NASA grant NAG5-9650 at U. C. Berkeley, NAG5-4408 and NAG5-6925 at the University of New Hampshire, NAG5-7185 at Dartmouth College, and NAG5-2371 at the University of Iowa.

References

André, R., M. Pinnock, and A. S. Rodger, On the SuperDARN autocorrelation function observed in the cusp, *Geophys. Res. Lett.*, **26**, 3353–3356, 1999.

Aubry, M. P., C. T. Russell, and M. G. Kivelson, Inward motion of the magnetopause before a substorm, *J. Geophys. Res.*, **75**, 7018–7031, 1970.

Axford, W. I. and C. O. Hines. A unifying theory of high-latitude geophysical phenomena and geomagnetic storms, *Canadian Journal of Physics*, **39**, 1433–1464, 1961.

Baker, K. B., J. R. Dudeney, R. A. Greenwald, M. Pinnock, P. T. Newell, A. S. Rodger, N. Mattin, and C.-I. Meng, HF radar signatures of the cusp and low-latitude boundary layer, *J. Geophys. Res.*, **100**, 7671–7695, 1995.

Burke, W. J., D. R. Weimer, and N. C. Maynard, Geoeffective interplanetary scale sizes derived from regression analysis of polar cap potentials, *J. Geophys. Res.*, **104**, 9989–9994, 1999.

Crooker, N. U., Dayside merging and cusp geometry, *J. Geophys. Res.*, **83**, 951–959, 1979.

Dungey, J. W., Interplanetary magnetic field and the auroral zones, *Phys. Rev. Lett.*, **6**, 47–48, 1961.

Fairfield, D. H., Average and unusual locations of the Earth's magnetopause and bow shock, *J. Geophys. Res.*, **76**, 6700, 1971.

Fornacon, K.-H. *et al.*, The magnetic field experiment onboard Equator-S and its scientific possibilities, *Ann. Geophysicae.*, **17**, 1521–1527, 1999.

Frank, L. A. *et al.*, The comprehensive plasma instrumentation (CPI) for the Geotail spacecraft, *J. Geomag. Geoelectr.*, **46**, 23–37, 1994.

Giovanelli, R. G., A theory of chromospheric flares, *Nature*, **158**, 81–82, 1946.

Gonzales, W. D. and F. S. Mozer, A quantitative model for the potential resulting from reconnection with an arbitrary interplanetary magnetic field, *J. Geophys. Res.*, **79**, 4186–4194, 1974.

Gosling, J. T. *et al.*, Accelerated plasma flows at the near-tail magnetopause, *J. Geophys. Res.*, **91**, 3029–3041, 1986.

Greenwald, R. A., K. B. Baker, J. R. Dudeney, M. Pinnock, T. B. Jones, E. C. Thomas, J.-P. Villain, J.-C. Cerisier, C. Senior, C. Hanuise, R. D. Hunsucker, G. Sofko, J. Koehler, E. Nielsen, R. Pellinen, A. D. M. Walker, N. Sato, and H. Yamagishi, DARN/SuperDARN: A global view of the dynamics of high-latitude convection, *Space Science Rev.*, **71**, 761–796, 1995.

Hudson, P. D., Discontinuities in an anisotropic plasma and their identification in the solar wind, *Planet. Space Sci.*, **18**, 1611, 1970.

Innes, D. E. *et al.*, Bi-directional plasma jets produced by magnetic reconnection on the Sun, *Nature*, **386**, 811–813, 1997.

Kistler, L. M. *et al.*, Testing Electric Field Models Using Ring Current Ion Energy Spectra from the Equator-S Ion Composition (ESIC) Experiment, *Ann. Geophys.*, **12**, 1611–1621, 1999.

Kokubun, S. *et al.*, The GEOTAIL magnetic field experiment, *J. Geomag. Geoelectr.*, **46**, 7, 1994.

Levy, R. H., H. E. Petschek, and G. L. Siscoe, Aerodynamic aspects of the magnetospheric flow, *AIAA J.*, **2**, 2065, 1964.

Masuda, S. *et al.*, A loop-top hard X-ray source in a compact solar flare as evidence for magnetic reconnection, *Nature*, **371**, 495–497, 1994.

Mukai, S. *et al.*, The Low Energy Particle (LEP) experiment onboard the GEOTAIL Satellite, *J. Geomag. Geoelectr.*, **46**, 669, 1994.

Niedner, M. B., J. A. Ionson, and J. C. Brandt, Interplanetary Gas. XXVI. On the reconnection of magnetic fields in cometary ionospheres at interplanetary sector boundary crossings, *Astrophys. J.*, **245**, 1159–1169, 1981.

Paschmann, G. *et al.*, Plasma acceleration at the earth's magnetopause: Evidence for reconnection, *Nature*, **282**, 243–246, 1979.

Paschmann, G. *et al.*, The magnetopause for large magnetic shear: AMPTE/IRM observations, *J. Geophys. Res.*, **91**, 11099, 1986.

Phan, T. D. *et al.*, Extended magnetic reconnection at the Earth's magnetopause from detection of bi-directional jets, *Nature*, **404**, 848–850, 2000.

Siscoe, G. L. and T. S. Huang, Polar cap inflation and deflation, *J. Geophys. Res.*, **90**, 543, 1985.

Sonnerup, B. U. Ö., The magnetopause reconnection rate, *J. Geophys. Res.*, **79**, 1546–1549, 1974.

Sonnerup, B. U. Ö. *et al.*, Evidence for reconnection at the earth's magnetopause, *J. Geophys. Res.*, **86**, 10049–10067, 1981.

Yokoyama, T. and K. Shibata, Magnetic field reconnection as the origin of X-ray jets and H-Alpha surges on the sun, *Nature*, **375**, 42, 1995.

T. D. Phan (e-mail: phan@ssl.berkeley.edu), M. P. Freeman, L. M. Kistler, B. Klecker, G. Haerendel, G. Paschmann, B. U. Ö. Sonnerup, W. Baumjohann, M. B. Bavassano-Cattaneo, C. W. Carlson, A. M. DiLellis, K.-H. Fornacon, L. A. Frank, M. Fujimoto, E. Georgescu, S. Kokubun, E. Moebius, T. Mukai, W. R. Paterson, and H. Reme